Cofactors are essential constituents of stable and seeding-active tau fibrils

Yann Fichou[a,1,2], Yanxian Lin[b,1], Jennifer N. Rauch[c,d], Michael Vigers[e], Zhikai Zeng[a], Madhur Srivastava[f], Timothy J. Keller[a], Jack H. Freed[f], Kenneth S. Kosik[c,d], and Songi Han[a,e,2]

[a]Department of Chemistry and Biochemistry, University of California, Santa Barbara, CA 93106; [b]Biomolecular Science and Engineering, University of California, Santa Barbara, CA 93106; [c]Molecular, Cellular and Developmental Biology, University of California, Santa Barbara, CA 93106; [d]Neuroscience Research Institute, University of California, Santa Barbara, CA 93106; [e]Department of Chemical Engineering, University of California, Santa Barbara, CA 93106; and [f]ACERT (National Biomedical Center for Advanced ESR Technology), Department of Chemistry and Chemical Biology, Cornell University, Ithaca, NY 14853

Amyloid fibrils are cross-β–rich aggregates that are exceptionally stable forms of protein assembly. Accumulation of tau amyloid fibrils is involved in many neurodegenerative diseases, including Alzheimer's disease (AD). Heparin-induced aggregates have been widely used and assumed to be a good tau amyloid fibril model for most biophysical studies. Here we show that mature fibrils made of 4R tau variants, prepared with heparin or RNA, spontaneously depolymerize and release monomers when their cofactors are removed. We demonstrate that the cross-β-sheet assembly formed in vitro with polyanion addition is unstable at room temperature. We furthermore demonstrate high seeding capacity with transgenic AD mouse brain-extracted tau fibrils in vitro that, however, is exhausted after one generation, while supplementation with RNA cofactors resulted in sustained seeding over multiple generations. We suggest that tau fibrils formed in brains are supported by unknown cofactors and inhere higher-quality packing, as reflected in a more distinct conformational arrangement in the mouse fibril-seeded, compared with heparin-induced, tau fibrils. Our study suggests that the role of cofactors in tauopathies is a worthy focus of future studies, as they may be viable targets for diagnosis and therapeutics.

tau | amyloid aggregates | seeding | aggregate cofactors | DEER

Amyloid aggregates are structured aggregates that are characterized by a high cross-β-sheet content. They rely on an extended intermolecular hydrogen-bond network that provides high stability, and allow even hydrophilic and charged domains to be dehydrated and tightly packed in a protein assembly (1). Amyloid aggregates have been conjectured to be the most stable form of protein assembly (2). The molecular forces from which this extreme stability originates were revealed mostly based on model peptides forming perfect cross-β-structures (3). However, many amyloid aggregates are only partially composed of amyloid cross-β-sheets, and likely do not possess the high stability of model peptides.

The tau protein is an intrinsically disordered protein that is mostly present in neurons and can form amyloid fibrils in several neurodegenerative diseases including Alzheimer's disease (AD), frontotemporal dementia, and Pick's disease (4). Tau is highly charged and hydrophilic, making it highly soluble and stable in aqueous environments across a wide range of pH and temperature. However, under pathological conditions, it can assemble into amyloid fibrils in which parts of its microtubule-binding domain, predominantly positively charged, densely pack into a cross-β-sheet arrangement (5). However, the triggering factors and driving forces of fibrillation of the highly soluble tau protein remain unknown, and consequently neither the mechanism that achieves convergence to a unique fibril structure nor the main fibril feature that contributes to its stability is understood.

Aggregation mechanisms are most often studied with recombinant tau proteins or fragments. In vitro fibrillation of tau is typically triggered with the help of cofactors, most commonly heparin (6), but also other cofactors such as RNA (7) or arachidonic acid (8). In the last few years, seeding tau aggregation has been shown to be possible by adding premade fibrils (seeds) to fresh monomers, but the seeding process is still improved by the presence of cofactors (RNA or heparin) in solution (9, 10). It has been shown that heparin is a limiting factor in fibril formation (11, 12), but the exact nature of association of heparin with the mature fibrils remains unclear, with conflicting reports on whether heparin is part of (13) or not part of mature fibrils (12, 14). As a result, the roles of heparin in tuning fibril formation, structure, and stability are unknown. For instance, heparin-induced fibrils were shown to be more stable than AD fibrils using chemical denaturation (15, 16), but whether heparin contributes to this stability was not addressed. In this study, we assess whether cofactors are crucial constituents of mature fibrils and contribute to their stability, or whether they only catalyze aggregation toward a self-sustained protein assembly.

Tau aggregates have been shown to propagate from neuron to neuron, and to be able to seed aggregation (16, 17), that is, convert naïve tau monomers into aggregates. This led to the hypothesis that, in vivo, monomeric tau can spontaneously polymerize into amyloid filaments when an appropriate seed template is provided. For that reason, pathological origins of tau aggregation have mostly been searched in the properties of tau itself, such as

Significance

The tau protein is involved in Alzheimer's and other neurodegenerative diseases, where the location, morphology, and quantity of amyloid fibrils composed of tau correlate with the disease type and stage. While tau fibrillary aggregates have been colocalized in brains together with several cofactors, their role in fibril formation, structure, and seeding has been largely neglected. We show that seeding of tau aggregation is facilitated by polyanionic cofactors, and that seeded or recombinant mature fibrils depolymerize into monomers when their cofactor is removed. We show that cofactor-assisted seeding with mouse brain-derived tau fibrils yielded tau fibrils with distinct and narrowed structural properties compared with heparin-induced fibrils, suggesting that the fibrillar templates tuned the structure of the seeded fibril.

BIOCHEMISTRY

BIOPHYSICS AND COMPUTATIONAL BIOLOGY

hyperphosphorylation, cleavage, high local concentrations, and alternative splicing, but marginally in abnormal interactions with other cofactors. Paradoxically, cofactors are always used for in vitro aggregation of tau, and even assumed to be biologically relevant. Therefore, gaining an understanding about the influence of cofactors on mature fibril properties will (i) provide key insight into the role of cofactors in fibril stability and conformation in vitro, and (ii) guide the search for cofactors that assist in seeding and spreading of tau aggregation in vivo. In this study, we used a set of biochemical tools together with electron paramagnetic resonance (EPR) to characterize the consequences of cofactor removal after fibril formation.

Results

Fibrils Assemble When Cofactors Are Present. We used a truncated version of the longest human tau isoform, 2N4R, that contains four repeat domains (R1 to R4), as well as the entire C-terminal region (residues 255 to 441, named here tau187), from which one of the two cysteines was mutated (C291S) to perform site-directed spin labeling for EPR (18, 19). The construct, with the addition of the aggregation-promoting disease mutation P301L (20), is referred to as tau throughout the manuscript (*SI Appendix*, Fig. S1*A*). Polydisperse heparin (average molecular mass 15 kDa) and polyU (RNA, average molecular mass 900 kDa) were incubated with tau to induce fibrillation. The addition of heparin or RNA to tau resulted in amyloid fibril formation, as verified by significant increase of thioflavin T (ThT) fluorescence intensity (*SI Appendix*, Fig. S2) and the presence of fibrillar structures captured by transmission electron microscopy (TEM; *SI Appendix*, Fig. S1 *B and C*). We refer to the heparin-induced and RNA-induced tau amyloid fibrils as heparin fibrils and RNA fibrils, respectively.

Fibrils Depolymerize When Cofactors Are Digested. We tested whether these cofactors act as catalysts that assist fibril formation and subsequently dissociate from the product, or whether they are reactants that are part of the fibril scaffold and are necessary to ensure the stability of mature fibrils. To address this question, we investigated amyloid fibril quantity by preparing heparin fibrils and RNA fibrils and then degrading the cofactors via enzymatic digestion.

Heparin and RNA are cofactors that can be digested using heparinase and RNase, respectively (*Methods and Materials*). In their digested form, both cofactors are incapable of triggering fibril formation (*SI Appendix*, Fig. S3). ThT fluorescence, which provides an in situ measure of cross-β-sheet structure abundance, was used to quantify the amyloid fibrils present in the sample. Heparinase and RNase were added to heparin fibrils and RNA fibrils after maximal ThT fluorescence was reached, and the samples were incubated for over 7 to 8 h, resulting in a 20 to 30% and 70 to 80% decrease of ThT fluorescence, respectively (Fig. 1*A*). Similar results were obtained when performing digestion on pelleted fibrils upon ultracentrifugation, showing that the decrease in ThT upon enzyme addition is not due to degradation of ThT-active soluble oligomers or fibrils (*SI Appendix*, Fig. S4). Control experiments with buffer added to heparin and RNA fibrils in the absence of enzymes showed ThT fluorescence decreases of ~10 and ~30%, respectively (Fig. 1*A*), which are attributed to result from dilution and potential traces of RNase.

The digestion of tau amyloid fibrils was further characterized by TEM (*SI Appendix*, Fig. S5). Both heparin and RNA fibril images showed no discernable population of oligomeric or protofibrillar aggregates neither before nor after digestion (*SI Appendix*, Fig. S5 *A–D*). A statistical analysis of the width of heparin fibrils was carried out before and after heparinase treatment. The distribution of fibril width (*SI Appendix*, Fig. S5 *E and F*) did not distinguish different fibril populations neither before nor after digestion, and the average measured width was found to be similar before (15.3 ± 3.9 nm) and after (14.9 ± 2.8 nm) digestion. Thus, within the resolution provided by TEM, no preferential fibril population subject to digestion could be identified.
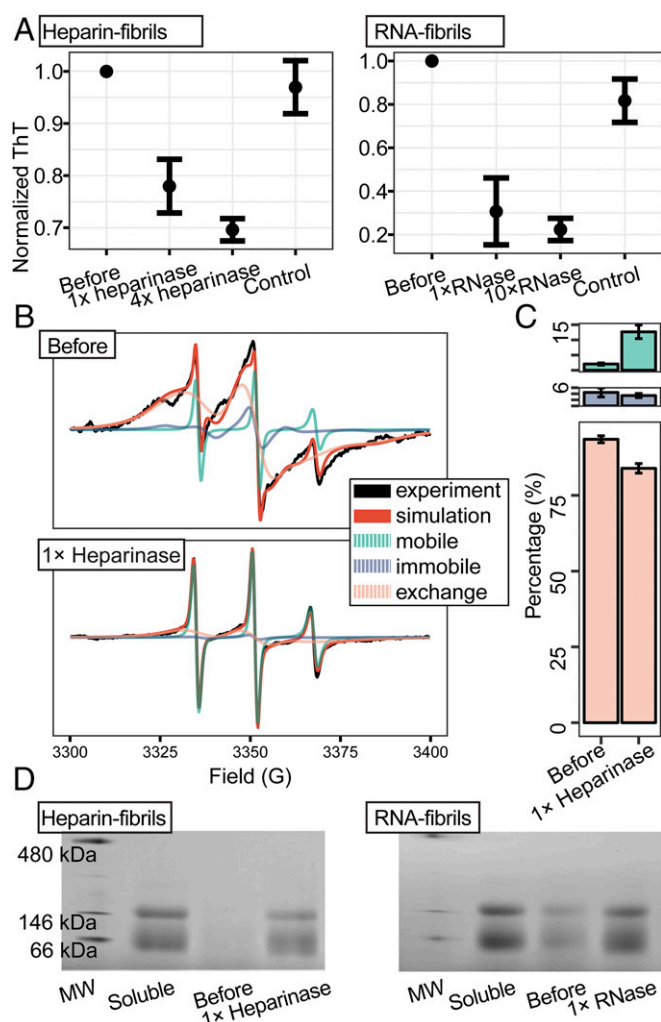
Fig. 1. Fibrils depolymerize upon cofactor digestion. (*A*) ThT fluorescence of heparin-induced tau fibrils and RNA-induced tau fibrils before and after incubation with different concentrations of heparinase/RNase. ThT fluorescence value measured before enzyme addition was used as the normalization value. (*B*) cw-EPR spectra (black) of tau heparin fibrils spin-labeled at site 322, before and after incubation with heparinase. The simulation spectra (red) are composed of mobile (green), immobile (purple), and spin-exchange components (orange). (*C*) Population of each component extracted from cw-EPR spectrum analysis. (*D*) BNPAGE of heparin and RNA fibrils before and after incubation. Freshly prepared tau monomers were loaded as reference (soluble). In all panels, 1× heparinase: 1 U enzyme per 1 μg heparin; 1× RNase: 2.5 μg/mL. Error bars show SD (*n* ≥ 3).

The digestion of tau amyloid fibrils was independently investigated by continuous-wave EPR (cw-EPR). cw-EPR of paramagnetic spins tethered to tau has been previously used to assess the packing and mobility of tau fibrils (18). The cw-EPR spectra of spin-labeled amyloid fibrils can be decomposed into three components: a mobile component corresponding to soluble low molecular mass species, an immobile component corresponding to high molecular mass species (oligomers, aggregates, etc.), and a spin-exchange component resulting from spin labels that are within 5-Å proximity due to parallel, in-register, amyloid cross-β-stacking of tau (18). Here we spin-labeled the native cysteine 322, prepared tau fibrils with heparin, and acquired cw-EPR spectra before and after heparinase treatment. The spectra were fitted using an established simulation protocol (18) into populations of mobile, immobile, and spin-exchange components (Fig. 1*B*). Fitting results implied that 93 ± 1% of the spin-labeled tau in heparin fibrils is in in-register amyloid cross-β-stacking, which

decreases to $84 \pm 2\%$ after digestion. This loss was mostly compensated by increase of low molecular mass species ($2 \pm 0.3\%$ before and $13 \pm 2\%$ after digestion), while the high molecular mass species remains similar ($4 \pm 1\%$ before and $3 \pm 1\%$ after digestion) (Fig. 1C).

The increase of low molecular mass species interpreted from cw-EPR after digestion was further tested for both heparin and RNA fibrils using blue native polyacrylamide gel electrophoresis (BNPAGE; Fig. 1D). The results showed that tau fibrils after digestion release a significant amount of solubilized monomer and dimer, in contrast to tau fibrils before digestion, where no corresponding band could be discerned. Note that the ratio of monomer/dimer remained unchanged for the sample before aggregation ("soluble" lane) and after digestion. These results are direct evidence confirming that the decrease of ThT fluorescence observed in Fig. 1A results from a depolymerization of tau fibrils.

Bound Cofactors Are Required to Stabilize Tau Fibrils. We learned that digesting cofactors depolymerized tau fibrils. However, extending the digestion for longer times or increasing heparinase and RNase concentration by 4 and 10 times, respectively, did not significantly decrease the remaining ThT fluorescence (Fig. 1A), which suggests that the maximal digestion had been reached and the remaining ThT fluorescence came from species that are not sensitive to heparinase/RNase digestion. These species can originate from either (i) fibril populations that are stable without a cofactor, or (ii) fibril populations stabilized by cofactors that are undigestible due to steric hindrance. To answer this question, we quantified the amount of undigested cofactor by separating the soluble cofactors from fibrils.

Mature RNA fibrils were pelleted, washed, and incubated with or without RNase, referred to as digested and nondigested RNA fibrils, respectively. Digested and nondigested RNA fibrils were subjected to dialysis, and the percentage of equilibrated RNA that flowed through the dialysis membrane was measured by UV absorption and regarded as effectively digested RNA. Digested and nondigested RNA (without tau) were used as controls. Results presented in Fig. 2B revealed a degree of RNA digestion of $81 \pm 2\%$ and $36 \pm 3\%$ for digested and nondigested RNA fibrils, respectively. These results confirm that the majority of the RNA in RNA fibrils was digested upon RNase treatment, while the small but significant difference between digested fibrils ($81 \pm 2\%$) and digested RNA alone ($90 \pm 4\%$) reveals that a fraction of the RNA in the fibrils is protected against digestion. The above difference of $9 \pm 6\%$ is in qualitative agreement with the remaining ThT fluorescence ($8 \pm 2\%$) observed after digestion of pelleted fibrils (*SI Appendix*, Fig. S4). Note that the $36 \pm 3\%$ of RNA flowed through in the nondigested fibrils is close to the nondigested RNA control ($28 \pm 5\%$), suggesting it originates mostly from RNase contamination inside the dialysis tube that digests RNA over the dialysis time of 24 h.

Heparin fibrils were prepared using spin-labeled heparin (heparin-SL), detectable by cw-EPR. The double integral of a cw-EPR spectrum is directly proportional to the quantity of spin label, and hence yields the heparin concentration. We first confirmed using a ThT assay that heparin-SL triggers tau fibrillation (*SI Appendix*, Fig. S6). Dialysis as a way of separating digested heparin from fibrils could not be applied because the dialysis membrane seemed to react with the heparin-SL, yielding unreliable results. Instead, digested and nondigested heparin-SL fibrils were subjected to filtration (0.2 μm) that allowed the soluble heparin to flow through, while retaining the large fibrils and associated heparin (Fig. 2A). The concentration of heparin in the filtrate was determined by cw-EPR and compared with the concentration before filtration to calculate the percentage of soluble heparin (Fig. 2B). Both digested and nondigested samples retained a significant amount of heparin ($42 \pm 8\%$ and $39 \pm 2\%$ flowed through, respectively), while the control with only heparin-SL (no tau fibrils) flowed entirely through ($108 \pm 6\%$). The observation that even after digestion a large portion of
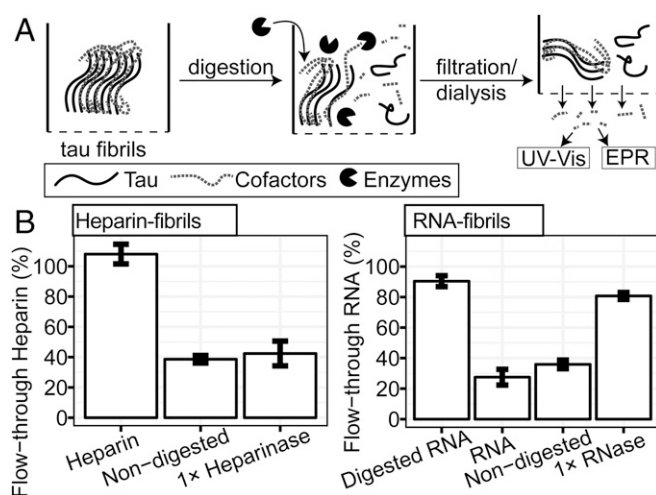
Fig. 2. Cofactors are bound to fibrils and partially digested. (A) Schematic diagram of experimental procedures. Digested soluble cofactors were separated from tau fibrils via dialysis (RNA fibrils) or filtration (heparin fibrils) before measuring their concentration in the flow-through by cw-EPR (heparin) or UV absorbance (RNA). (B, Left) The concentration of spin-labeled heparin in the flow-through of a 0.2-μm filter for heparin and heparin fibrils before and after digestion. The concentration is given as the percentage of the concentration before filtration. (B, Right) RNA concentration outside a dialysis bag (12 kDa molecular mass cutoff) at equilibrium was measured and the percentage of RNA that flowed through is given on the y axis. Error bars show SD of three independent repeats.

heparin is bound to fibrils is in qualitative agreement with the ThT fluorescence that retains 80% of its intensity after digestion (Fig. 1A). We however could not detect a significant difference between digested and undigested samples, in part due to the large variation in the measurement of spin concentration ($\pm 8\%$ for the digested sample).

Furthermore, we detected a reproducible change in EPR lineshape of heparin-SL upon fibril formation. We report in *SI Appendix*, Fig. S7, *Inset* the width of the central peak before aggregation, after aggregation, and after digestion. A broadening of the central peak, implying slowed dynamics of the spin labels, was observed upon aggregation. These results are consistent with the picture that (i) heparin is bound to fibril (line broadening between before and after aggregation), (ii) heparinase digestion detaches some heparin from the fibrils (line narrowing between before and after digestion), and (iii) the remaining heparinase-resistant fibrils still contain bound heparin (broadening after pelleting the digested fibers). Taken together, the quantification of cofactors as well as the cw-EPR lineshapes of heparin-SL strongly suggest that fibrils remaining after enzymatic digestion are stabilized by cofactors that are still associated with the fibrils and could not be digested (the second of the two posited scenarios).

Depolymerized Tau Monomers Have No "Memory" of the Fibril State. Tau undergoes drastic conformational rearrangements upon aggregation. We tested whether the released monomers after digestion recovered their original properties by measuring their conformational feature, their capacity to reform fibrils, as well as their capacity to seed aggregation.

We first tested whether or not released tau monomers were able to reaggregate. RNA fibrils were pelleted before digestion to ensure that only insoluble fibrils were subjected to digestion. The digested RNA fibrils were filtered and loaded onto a size-exclusion chromatography (SEC) column to purify the released monomers. The aggregation of these released monomers was then compared with freshly prepared monomers (i.e., that did not go through the fibril state) at an identical concentration. ThT fluorescence presented in Fig. 3A showed that both fresh monomers and digested monomers displayed similar aggregation

kinetics and maximal quantity. Note that heparin was used for this reaggregation experiment because of the difficulty of reliably removing RNase, even with SEC.

The reaggregation assay of heparin fibrils was slightly different because heparinase did not release enough monomers to rely on SEC purification. Instead, heparinase was inactivated by heating the sample at 65 °C for 15 min. We then added fresh heparin at a tau:hepari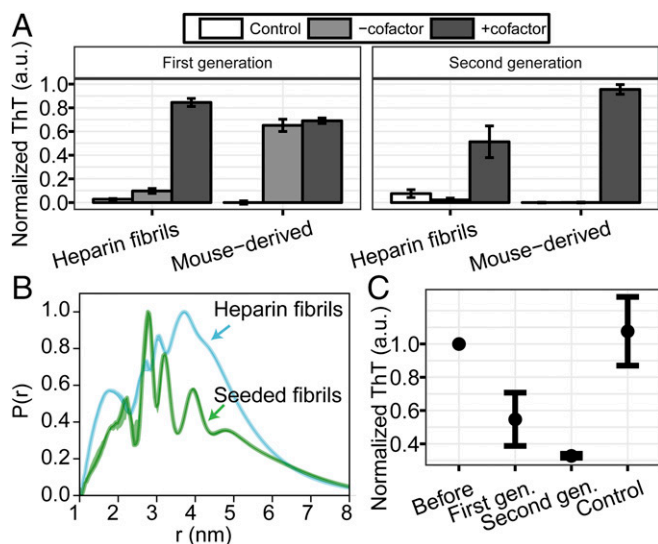n molar ratio of 10:1 to both digested and nondigested heparin fibrils (predigested fibrils and nondigested fibrils, respectively, in Fig. 3A). The change of ThT fluorescence was recorded and normalized to a scale from 0 to 1. Upon addition of heparin, the ThT fluorescence increased significantly more in the digested sample than in the nondigested sample, showing that the released monomers can reaggregate. The small increase in the nondigested sample might originate from the reaggregation of monomers that were released when heating the sample at 65 °C.

The conformational features associated with fibril digestion were further investigated. We have previously identified a signature of aggregation-prone tau conformations represented by a dramatic conformational extension around the amyloidogenic hexapeptides PHF6 (^{306}VQIVYK^{311}) and PHF6* (^{275}VQIINK^{280}) (21). Following a similar procedure as shown in Eschmann et al. (21), we measured the distribution of intratau spin-label distance, r, spanning residues 272 and 285 by double electron–electron resonance (DEER). The distance distribution, $P(r)$, was determined using the recently developed picard-selected segment-optimized (PICASSO) singular value decomposition (SVD) of the time-domain DEER decay (22, 23). We first confirmed the expected distance extension around PHF6* when

transitioning from monomer to heparin fibrils (Fig. 3B). The releasing of tau monomer upon heparinase treatment resulted in the partial reversal of the PHF6* distance extension (Fig. 3B), showing that the released tau lost its aggregation-prone conformational signature of solvent-exposed PHF6*. The $P(r)$ of the digested sample showed distinct features containing signatures of both the PHF6*-protected conformation (e.g., peak at 2.2 nm) and the PHF6*-exposed conformation (population at $r > 4$ nm), indicating the coexistence of both fibril and released monomers.

It was recently proposed that after aggregation, tau, even in its monomeric form, maintains aggregate-templated conformations that provide high seeding capacities (24). According to this hypothesis, the aggregation propensity of the tau monomers released from the digested fibrils should be much higher than that of fresh tau monomers, as the released monomers would populate fibrillation-prone conformations with increased numbers of nucleation sites in the sample. We tested this hypothesis by measuring the seeding propensity of heparin and RNA fibrils before and after cofactor digestion, both in vitro and in vivo. We used a cellular seeding assay similar to previously established assays (25, 26) in H4 neuroglioma. When the overexpressed proteins aggregate, they form fluorescent puncta (25) due to the fluorescent protein mCerulean tethered to tau (*SI Appendix*, Fig. S8). Fig. 3C reports the percentage of cells that exhibited puncta. While all samples triggered seeding, there were no significant differences between digested and nondigested fibrils, suggesting that the monomers released from fibrils are not seeding-active. Furthermore, seeding was only possible when the fibrils were mildly sonicated (*SI Appendix*, Fig. S9A). We interpreted this observation by suggesting that breaking the fibril is necessary for its efficient uptake, which again showed that monomers are not the active seeding species. The same results were obtained with H4 cells expressing tau187 instead of K18 (*SI Appendix*, Fig. S9B). Furthermore, we tested the seeding capacity of heparin fibrils in an in vitro assay where the premade fibrils were added to fresh monomers in the presence or absence of a cofactor (see next section for precise assay description). *SI Appendix*, Fig. S10 shows that digested fibrils have lower seeding capacity compared with intact fibrils, as demonstrated with a smaller increase in ThT fluorescence (compare green with cinnamon curves). This result is in good agreement with the idea that depolymerized monomers do not seed aggregation, and that the loss of seeding capacity is due to the loss of fibril content after cofactor digestion. The monomers derived from fibrils have no memory of the fibril state, neither in conformation nor in seeding capacity.

The Presence of Cofactor Sustains Fibril Seeding. To test the role of cofactors in seeding/spreading of fibrillation, we performed in vitro seeding assays of tau over two generations with and without cofactors, using either mouse-derived fibrils or heparin fibrils as seeds. The same tau construct as before was used, tau187C291S, but without the aggregation-promoting P301L mutation. We made this choice, as this tau variant is incapable of spontaneous fibril formation with RNA (*SI Appendix*, Fig. S11). Five percent (mass) of heparin fibrils were added as seeds to fresh tau in the presence or absence of RNA cofactor (polyU) while ThT fluorescence was monitored. Fig. 4A presents the ThT fluorescence of the seeding experiments after 10 h, while the full aggregation curves are shown in *SI Appendix*, Fig. S12. The presence of the RNA cofactor significantly increased the seeding capacity of both digested and nondigested heparin-fibril seeds. For second-generation seeding, 10% of the end product of the first generation was added to the fresh monomers, with or without cofactor (Fig. 4A). As for first-generation seeding, the presence of cofactor significantly enhanced the seeding activity. The same experiments were carried out using mouse-derived fibril (rTg4510 mice expressing 2N4R-P301L) seeds (Fig. 4A). In contrast, the presence of a cofactor did not change the seeding capacity of mouse-derived fibrils in the first generation (Fig. 4A). For second-generation seeding, where 10% end product of the first-generation sample was used as the new seed, aggregation

Fig. 3. Refibrillization and conformation recovery of depolymerized tau monomers. (A, Left) ThT fluorescence of non/predigested heparin fibrils after heparin addition at time $t = 0$ h. (A, Right) Aggregation of monomers purified from digested RNA fibrils compared with fresh monomers. Curves of the same color show independent repeats. (B) DEER time-domain signal (Left) and corresponding distance distributions (Right), extracted with the SVD method, of tau labeled at residues 272 and 285 before and after digestion, compared with soluble monomer. (C) Quantification of in vivo seeding experiments. The ratios of cells that contain fluorescent puncta are reported. Digst, digested; fib, fibrils; Hep, heparin.

Fig. 4. In vitro seeding of tau fibrils. (*A*) ThT fluorescence of recombinant tau187C291S seeded with heparin fibrils or mouse-derived fibrils (mouse-derived) in the presence or absence of cofactor (polyU RNA). In first-generation seeding (*Left*), 5% of preaggregated fibrils were added to fresh recombinant tau and incubated at 37 °C while shaking. In the second generation (*Right*), 10% of the end products of first-generation samples were added to fresh monomers. Control refers to the seeds with cofactor incubated without fresh tau. Error bars shows SD (*n* = 3). (*B*) DEER distance distribution between residues 272 and 285 of heparin fibrils and mouse-derived seeded fibrils (seeded fibrils) obtained from the SVD method. (*C*) ThT fluorescence before and after RNase addition to the first and second generations of mouse-derived seeded fibrils. Error bars shows SD (*n* ≥ 3). gen, generation.

was observed only when a cofactor was supplied (Fig. 4*A*). The aggregation kinetics appeared to be slower compared with the other seeding experiment, as the ThT signal had not plateaued after 10 h. Altogether, the results presented in Fig. 4 show that cofactors are needed to promote templated seeding, and suggested that unknown cofactor species are present in mouse-derived material, which facilitated first-generation seeding without an extrinsic cofactor, while the second-generation fibrils were incapable of seeding, unless extrinsic cofactors were added.

To test whether seeding with mouse-derived material impacted the structure of the seeded tau fibrils, we performed DEER of doubly labeled tau187 at residues 272 and 285 (same sites as in Fig. 3*B*), whose aggregation was seeded with mouse-derived fibrils in the presence of polyU RNA cofactor (1% seed). The distance distribution was obtained using PICASSO (22) and compared with that of heparin fibrils (Fig. 4*B*). The *P*(*r*)s are significantly different, implying that seeded and heparin-induced fibrils are structurally different, where specifically the seeded fibrils showed distinctly narrowed peaks reflecting multiple, highly ordered, fibril populations. In contrast, heparin-induced fibrils exhibited broader *P*(*r*) features that represent imperfectly packed (at least locally around PHF6*) fibrils populating a continuum of distances. This result agrees with the view that in vivo tau aggregates populate specific tau strains (27) that are structurally well-defined (5), while heparin fibrils are highly heterogeneous (28). This result shows at high resolution a structural convergence of recombinant fibrils guided by mouse-derived fibrils, suggesting that in vivo aggregates can transmit their structural properties to naïve tau by templated seeding. When the just-discussed mouse-seeded fibrils, formed in the presence of polyU cofactor, were subjected to RNase treatment, again a partial decay of the ThT signal was observed (Fig. 4*C*), implying that the loss of β-sheet packing also occurs when the fibrils are structurally templated by mouse-extracted fibrils, underscoring the importance of the presence and nature of the cofactor.

Discussion

We have demonstrated that mature recombinant tau fibrils require cofactors to be sustainably stable. Upon cleavage of cofactors by enzymatic digestion, the fibrils depolymerize, releasing soluble monomeric tau. The incomplete digestion of the cofactor molecules (heparin or RNA) is likely due to allosteric hindrance that prevents the enzymes from accessing and cleaving their targets. The finding that in both RNA and heparin fibrils only a defined and reproducible amount of cofactor can be digested suggests that the fibrils are polymorphic, where in some types of aggregates the cofactors are protected from digestion while in others they are accessible to the enzyme. Note that single-point mutations change the extent to which ThT fluorescence is lost upon cofactor digestion (*SI Appendix*, Fig. S13), suggesting that the mutations affect the tau conformational ensemble within the fibril structure, and therefore the accessibility to the cofactors. The significant difference seen in Fig. 1*A* between the maximum digestible RNA (60 to 70%) and heparin (∼20%) could be explained by different molecular arrangements of the fibrils and/or by the nature of the enzymes, where RNase A (14 kDa) may be less sensitive to steric hindrance than heparinase I (43 kDa) to process its target.

Our work suggests that the high stability of heparin-induced fibrils previously observed (15, 16) is largely due to tau–cofactor interactions, and not due to superior tau fibril packing and stability. This highlights the need to further understand the role of cofactors in tuning the properties of tau fibrils of structure, stability, and seeding capacity.

The finding that a polyelectrolyte cofactor is essential for the stability of fibrils prepared in vitro has two major potential implications with respect to in vivo aggregates. (*i*) Polyanion-induced recombinant tau fibrils make limited models (of in vivo aggregates) that overestimate the role of the cofactor, and (*ii*) there is an unknown cofactor in the fibrils formed in neurons, whose roles have been underestimated to date. While we cannot rule out (*i*), the data presented here make a strong case for (*ii*).

We have successfully performed in vitro seeding of recombinant protein with heparin-induced fibrils and mouse brain-derived fibrils. Without providing additional cofactors, no significant seeding was observed with heparin-induced tau seeds, but the seeding capacity of brain-extracted fibril seeds was high (Fig. 4*A*), in agreement with previous work (16, 29). When fibrils extracted from this successful seeding experiment were used as pristine seeds for a second-generation seeding, no fibrils were formed (Fig. 4*D*), showing limited propagation of mouse-extracted fibrils through seeding. However, when a cofactor (polyU RNA) was provided in the reaction buffer, mouse-derive seeds, as heparin-induced seeds, were made competent over multiple generations (Fig. 4*A*). This result is in good agreement with the hypothesis that an unknown cofactor is present in the mouse-extracted aggregates that permits first-generation seeding, but not subsequent generations, as the cofactor present in the original seed gets consumed. In contrast, when a cofactor is provided in the buffer, seeding can be sustainably carried out over successive generations, as previously reported (10).

Fibrils seeded with mouse-extracted fibrils in the presence of RNA populated better-defined fibril structures compared with heparin fibrils (Fig. 4*B*), but they too could be partially digested (Fig. 4*C*), showing that RNA gets incorporated into the seeded fibrils. Interestingly, ∼45% of the ThT intensity is lost in the digestion of the first generation aided by RNA, while ∼70% of the ThT signal is lost in the second generation, approaching the level of digestion of RNA fibrils (Fig. 1*A*). This is in good agreement with the view that in the first generation, aggregation is partially aided by the unknown cofactor from the mouse fibrils that is insensitive to RNase, while in the second generation mostly extrinsic RNA is supporting the structures of the fibrils that are subject to the same levels of degradation as the non-seeded RNA-induced fibrils. Consistent with this picture is the observation that the mouse-extracted seed without the added RNA cofactor is completely insensitive to RNase (*SI Appendix*,

Fig. S14) and is degraded by neither DNase nor heparinase I (*SI Appendix*, Fig. S14). Studies to determine the stoichiometry and nature of the unknown cofactor originating from the brain-extracted seed will be timely.

There is a large variety of bioelectrolytes that could interact with tau in vivo, including DNA, RNA, glycoaminoglycan (GAG), and ATP. Although tau is mostly present in axons (30), it is also found in neuronal nuclei (31) and is suspected to traffic in the extracellular matrix (32). The complexity of the cellular environment and trafficking makes it very hard to unambiguously assess in situ the roles of a given cofactor in tau aggregation and the pathogenicity. GAG, in particular heparan sulfate (HS), has been the most studied interaction partner to tau [see, for instance, a recent review (33)], likely because (*i*) it was found colocalized with tau neurofibrillary tangles (NFTs) in AD brain (6), (*ii*) heparin is a very efficient cofactor in promoting aggregation in vitro (6), and (*iii*) HS has been shown to play an important role in tau internalization (34). Although it is unclear when and how HS interacts with tau, as the former is exclusively present on the extracellular surface while the latter is mainly found in the cytoplasm, the fact that the NFTs colocalize with HS (6) suggests that HS might be incorporated into in vivo tau fibrils. Similarly, RNA has also been found to specifically associate with tau in neurons (35), to be sequestered in tau pathological assemblies, not only in AD brains but also in Pick bodies (36), suggesting that RNA might also be part of the final tau fibrils. Recent advances in cryo-EM have allowed the identification of two very different fibril structures in AD brains (5) and Pick's disease (37), showing that different strains have very distinct atomistic fibril structures. If polyelectrolyte cofactors were present in the mature tau aggregates, they would not necessarily be visible on a cryo-EM electron density map (their high flexibility would likely compromise their resolution), while their interactions with tau could in fact modulate the differentiation toward a given strain.

Materials and Methods

A truncation of the longest human tau isoform, 2N4R, representing residues 255 to 441 was used throughout this work. Except when otherwise stated, this fragment possessed the mutations C291S and P301L and was referred to as tau throughout this manuscript. Fibrils were made by incubating 100 μM tau with 300 μg/mL polyU (RNA fibrils) or 20 μM tau with 5 μM heparin (heparin fibrils).

When aggregation was complete (maximum ThT intensity was observed), 2.5 μg/mL RNase A was added to digest RNA fibrils, and 1 U bacteroides heparinase I per 1 μg heparin was added to digest heparin-induced fibrils. These concentrations are denoted as 1× throughout the manuscript, while 2× represents twice these concentrations, and so forth. Thioflavin T was added in the buffers, and fluorescence was measured to follow aggregation. See *SI Appendix* for more details.

1. Greenwald J, Riek R (2010) Biology of amyloid: Structure, function, and regulation. *Structure* 18:1244–1260.
2. Jahn TR, Radford SE (2005) The yin and yang of protein folding. *FEBS J* 272:5962–5970.
3. Knowles TP, et al. (2007) Role of intermolecular forces in defining material properties of protein nanofibrils. *Science* 318:1900–1903.
4. Mandelkow EM, Mandelkow E (2012) Biochemistry and cell biology of tau protein in neurofibrillary degeneration. *Cold Spring Harb Perspect Med* 2:a006247.
5. Fitzpatrick AWP, et al. (2017) Cryo-EM structures of tau filaments from Alzheimer's disease. *Nature* 547:185–190.
6. Goedert M, et al. (1996) Assembly of microtubule-associated protein tau into Alzheimer-like filaments induced by sulphated glycosaminoglycans. *Nature* 383:550–553.
7. Kampers T, Friedhoff P, Biernat J, Mandelkow EM, Mandelkow E (1996) RNA stimulates aggregation of microtubule-associated protein tau into Alzheimer-like paired helical filaments. *FEBS Lett* 399:344–349.
8. Wilson DM, Binder LI (1997) Free fatty acids stimulate the polymerization of tau and amyloid beta peptides. In vitro evidence for a common effector of pathogenesis in Alzheimer's disease. *Am J Pathol* 150:2181–2195.
9. Dinkel PD, Holden MR, Matin N, Margittai M (2015) RNA binds to tau fibrils and sustains template-assisted growth. *Biochemistry* 54:4731–4740.
10. Meyer V, Dinkel PD, Rickman Hager E, Margittai M (2014) Amplification of tau fibrils from minute quantities of seeds. *Biochemistry* 53:5804–5809.
11. Ramachandran G, Udgaonkar JB (2011) Understanding the kinetic roles of the inducer heparin and of rod-like protofibrils during amyloid fibril formation by tau protein. *J Biol Chem* 286:38948–38959.
12. Carlson SW, et al. (2007) A complex mechanism for inducer mediated tau polymerization. *Biochemistry* 46:8838–8849.
13. Sibille N, et al. (2006) Structural impact of heparin binding to full-length tau as studied by NMR spectroscopy. *Biochemistry* 45:12560–12572.
14. von Bergen M, et al. (2006) The core of tau-paired helical filaments studied by scanning transmission electron microscopy and limited proteolysis. *Biochemistry* 45:6446–6457.
15. Morozova OA, March ZM, Robinson AS, Colby DW (2013) Conformational features of tau fibrils from Alzheimer's disease brain are faithfully propagated by unmodified recombinant protein. *Biochemistry* 52:6960–6967.
16. Falcon B, et al. (2015) Conformation determines the seeding potencies of native and recombinant tau aggregates. *J Biol Chem* 290:1049–1065.
17. Woerman AL, et al. (2016) Tau prions from Alzheimer's disease and chronic traumatic encephalopathy patients propagate in cultured cells. *Proc Natl Acad Sci USA* 113:E8187–E8196.
18. Pavlova A, et al. (2016) Protein structural and surface water rearrangement constitute major events in the earliest aggregation stages of tau. *Proc Natl Acad Sci USA* 113:E127–E136.
19. Hubbell WL, Altenbach C (1994) Investigation of structure and dynamics in membrane proteins using site-directed spin labeling. *Curr Opin Struct Biol* 4:566–573.
20. Mirra SS, et al. (1999) Tau pathology in a family with dementia and a P301L mutation in tau. *J Neuropathol Exp Neurol* 58:335–345.
21. Eschmann NA, et al. (2017) Signature of an aggregation-prone conformation of tau. *Sci Rep* 7:44739.
22. Srivastava M, Freed JH (2017) Singular value decomposition method to determine distance distributions in pulsed dipolar electron spin resonance. *J Phys Chem Lett* 8:5648–5655.
23. Srivastava M, Georgieva ER, Freed JH (2017) A new wavelet denoising method for experimental time-domain signals: Pulsed dipolar electron spin resonance. *J Phys Chem A* 121:2452–2465.
24. Mirbaha H, et al. (2018) Inert and seed-competent tau monomers suggest structural origins of aggregation. *eLife* 7:e36584.
25. Sanders DW, et al. (2014) Distinct tau prion strains propagate in cells and mice and define different tauopathies. *Neuron* 82:1271–1288.
26. Holmes BB, et al. (2014) Proteopathic tau seeding predicts tauopathy in vivo. *Proc Natl Acad Sci USA* 111:E4376–E4385.
27. Kaufman SK, et al. (2016) Tau prion strains dictate patterns of cell pathology, progression rate, and regional vulnerability in vivo. *Neuron* 92:796–812.
28. Fichou Y, Vigers M, Goring AK, Eschmann NA, Han S (2018) Heparin-induced tau filaments are structurally heterogeneous and differ from Alzheimer's disease filaments. *Chem Commun (Camb)* 54:4573–4576.
29. Guo JL, et al. (2016) Unique pathological tau conformers from Alzheimer's brains transmit tau pathology in nontransgenic mice. *J Exp Med* 213:2635–2654.
30. Xia D, Gutmann JM, Götz J (2016) Mobility and subcellular localization of endogenous, gene-edited tau differs from that of over-expressed human wild-type and P301L mutant tau. *Sci Rep* 6:29074.
31. Sultan A, et al. (2011) Nuclear tau, a key player in neuronal DNA protection. *J Biol Chem* 286:4566–4575.
32. Yamada K (2017) Extracellular tau and its potential role in the propagation of tau pathology. *Front Neurosci* 11:667.
33. Maïza A, et al. (May 4, 2018) The role of heparan sulfates in protein aggregation and their potential impact on neurodegeneration. *FEBS Lett*, 10.1002/1873-3468.13082.
34. Rauch JN, et al. (2018) Tau internalization is regulated by 6-O sulfation on heparan sulfate proteoglycans (HSPGs). *Sci Rep* 8:6382.
35. Zhang X, et al. (2017) RNA stores tau reversibly in complex coacervates. *PLoS Biol* 15:e2002183.
36. Ginsberg SD, et al. (1998) RNA sequestration to pathological lesions of neurodegenerative diseases. *Acta Neuropathol* 96:487–494.
37. Falcon B, et al. (2018) Structures of filaments from Pick's disease reveal a novel tau protein fold. *Nature* 561:137–140.